

Corroles with Group 15 Metal Ions. Synthesis and Characterization of Octaethylcorroles Containing As, Sb, and Bi Ions in +3, +4, and +5 Oxidation States

Karl M. Kadish,^{*,†} Christoph Erben,^{‡,§} Zhongping Ou,[†] Victor A. Adamian,^{†,||} Stefan Will,[‡] and Emanuel Vogel^{*,‡}

Department of Chemistry, University of Houston, Houston, Texas 77204-5641, and Institut für Organische Chemie, Universität zu Köln, Greinstrasse 4, 50939 Köln, Germany

Received November 23, 1999

The synthesis, spectroscopic characterization, and electrochemistry of As, Sb, and Bi corroles are reported. The investigated complexes are represented by [(OEC)As^V(CH₃)⁺ClO₄⁻ and (OEC)M where M = As(III), Sb(III), or Bi(III) and OEC is the trianion of octaethylcorrole. The products of each redox reaction are characterized by UV–vis and ESR spectroscopy. The first one-electron oxidations of (OEC)As and (OEC)Sb are metal-centered and result in the formation of [(OEC)As^{IV}]⁺ and [(OEC)Sb^{IV}]⁺. A second one-electron oxidations generates [(OEC)As^V]²⁺ and [(OEC*)Sb^{IV}]²⁺, the latter of which is slowly converted to a Sb(V) corrole, [(OEC)Sb^V]²⁺. The first one-electron oxidation of (OEC)Bi leads only to the Bi(III) π -cation radical, but a second one-electron oxidation is proposed to give a Bi(IV) complex, [(OEC)Bi]²⁺. The first reduction of [(OEC)As^V(CH₃)⁺ClO₄⁻ is accompanied by loss of the σ -bonded methyl ligand and formation of an As(III) complex.

Introduction

A number of metallocorroles containing transition metal central ions have been synthesized over the last 30 years.^{1–12} These compounds possess several properties quite different from those of the structurally related metalloporphyrins. Among the most important of these properties is the ability of the corrole macrocycle to stabilize higher oxidation states of the metal ion than is possible in the corresponding metalloporphyrins, and this is most evident in the case of several σ -bonded complexes such as (OEC)Fe(C₆H₅)⁷ and (OEC)Co(C₆H₅)⁸ (where OEC is

the trianion of octaethylcorrole), which contain formally tetravalent central metal ions in their air-stable form. Other corroles with high-valent metal ions are (OEC)Fe^{IV}Cl,^{6,10} (Et₄Me₄C)Cu,⁹ and (Et₄Me₄C)Ni⁹ (where Et₄Me₄C is the trianion of tetraethyltetramethylcorrole), the last two of which formally contain a trivalent metal ion. Another particular feature of the metallocorroles is their ability to readily undergo three macrocycle-centered oxidations,^{1,6–8} which contrasts with the two one-electron ring-centered oxidations seen for almost all metalloporphyrins.¹³

There is significant information in the literature on the synthesis, structure, spectroscopy, and electrochemistry of transition metal corroles, and numerous comparisons have been made between corroles and porphyrins containing the same central metal ion.^{1,2} In contrast, there are only a few examples in the literature of metallocorroles containing main group central ions, and these are limited to a series of octaalkylcorroles with In, Ge, and Sn central metals.^{1,2,14,15} There is only one report of metallocorroles containing group 15 elements as central ions¹⁶ as compared to a much larger number of published studies on porphyrins containing group 15 elements.^{17–29}

[†] University of Houston.

[‡] Universität zu Köln.

[§] Current address: Lucent Technologies—Bell Laboratories, Murray Hill, NJ, 07974.

^{||} Current address: BP Amoco Chemicals MC E-1B, 150 West Warrenville Rd., Naperville, IL 60563.

- (1) Erben, C.; Will, S.; Kadish, K. M. In *The Porphyrin Handbook*; Kadish, K. M., Smith, K. M., Guillard, R., Eds.; Academic Press: Burlington, MA, 2000; Vol. 2, pp 233–300.
- (2) Paolesse, R. In *The Porphyrin Handbook*; Kadish, K. M., Smith, K. M., Guillard, R., Eds.; Academic Press: Burlington, MA, 2000; Vol. 2, pp 201–232.
- (3) Genokhova, N. S.; Melent'eva, T. A.; Berezovskii, V. M. *Russ. Chem. Rev. (Engl. Transl.)* **1980**, *49*, 1056.
- (4) Melent'eva, T. A. *Russ. Chem. Rev. (Engl. Transl.)* **1983**, *52*, 641.
- (5) Licocchia, S.; Paolesse, R. *Struct. Bonding* **1995**, *84*, 71.
- (6) Autret, M.; Will, S.; Van Caemelbecke, E.; Lex, J.; Gisselbrecht, J.-P.; Gross, M.; Vogel, E.; Kadish, K. M. *J. Am. Chem. Soc.* **1994**, *116*, 9141.
- (7) Van Caemelbecke, E.; Will, S.; Autret, M.; Adamian, V. A.; Lex, J.; Gisselbrecht, J.-P.; Gross, M.; Vogel, E.; Kadish, K. M. *Inorg. Chem.* **1996**, *35*, 184.
- (8) Will, S.; Lex, J.; Vogel, E.; Adamian, V. A.; Van Caemelbecke, E.; Kadish, K. M. *Inorg. Chem.* **1996**, *35*, 5577.
- (9) Will, S.; Lex, J.; Vogel, E.; Schmickler, H.; Gisselbrecht, J.-P.; Hauptmann, C.; Bernard, M.; Gross, M. *Angew. Chem., Int. Ed. Engl.* **1997**, *36*, 357; *Angew. Chem.* **1997**, *109*, 367.
- (10) Vogel, E.; Will, S.; Schulze Tilling, A.; Neumann, L.; Lex, J.; Bill, E.; Trautwein, A. X.; Wieghardt, K. *Angew. Chem., Int. Ed. Engl.* **1994**, *33*, 731; *Angew. Chem.* **1994**, *106*, 771.
- (11) Licocchia, S.; Morgante, E.; Paolesse, R.; Polizio, F.; Senge, M. O.; Tondello, E.; Boschi, T. *Inorg. Chem.* **1997**, *36*, 1564.
- (12) Kadish, K. M.; Adamian, V. A.; Van Caemelbecke, E.; Gueletii, E.; Will, S.; Erben, C.; Vogel, E. *J. Am. Chem. Soc.* **1998**, *120*, 11986.

- (13) Kadish, K. M.; Royal, G.; Van Caemelbecke, E.; Gueletti, L. In *The Porphyrin Handbook*; Kadish, K. M., Smith, K. M., Guillard, R., Eds.; Academic Press: Burlington, MA, 2000; Vol. 9, pp 1–219.
- (14) Kadish, K. M.; Will, S.; Adamian, V. A.; Walther, B.; Erben, C.; Ou, Z.; Guo, N.; Vogel, E. *Inorg. Chem.* **1998**, *37*, 4573.
- (15) Paolesse, R.; Licocchia, S.; Boschi, T. *Inorg. Chim. Acta* **1990**, *178*, 9.
- (16) Paolesse, R.; Boschi, T.; Licocchia, S.; Khoury, R. G.; Smith, K. M. *J. Chem. Soc., Chem. Commun.* **1998**, 1119.
- (17) Treibs, A. *Liebigs Ann. Chem.* **1969**, *728*, 115.
- (18) Sayer, P.; Gouterman, M.; Connell, C. R. *Acc. Chem. Res.* **1982**, *15*, 73.
- (19) Sayer, P.; Gouterman, M.; Connell, C. R. *J. Am. Chem. Soc.* **1977**, *99*, 1082.
- (20) Knör, G.; Vogler, A. *Inorg. Chem.* **1994**, *33*, 314.
- (21) Liu, Y. H.; Bénassy, M.-F.; Chojnacki, S.; D'Souza, F.; Barbour, T.; Belcher, W. J.; Brothers, P. J.; Kadish, K. M. *Inorg. Chem.* **1994**, *33*, 4480.
- (22) Akiba, K.-y.; Onzuka, Y.; Itagaki, M.; Hirota, H.; Yamamoto, Y. *Organometallics* **1994**, *13*, 2800.
- (23) Kadish, K. M.; Autret, M.; Ou, Z.; Akiba, K.-y.; Masumoto, S.; Wada, R.; Yamamoto, Y. *Inorg. Chem.* **1996**, *35*, 5564.

In this paper, we report the synthesis, spectroscopic characterization, and electrochemistry of four new metallocorroles containing three different group 15 elements: (OEC)As, (OEC)-Sb, (OEC)Bi, and [(OEC)As(CH₃)⁺ClO₄⁻]. The products of electrooxidation and/or electroreduction are characterized by UV-vis and ESR spectroscopy, and an overall oxidation/reduction mechanism is proposed.

Experimental Section

Instrumentation. ¹H and ¹³C NMR spectra were recorded respectively at 300 and 75.5 MHz on a Bruker AP 300 NMR spectrometer. The solvent signals were used as standards at $\delta = 7.24$ (¹H) and $\delta = 77.0$ (¹³C). ESR spectra were recorded on an IBM ER 100D or on a Bruker ESP 380E spectrometer. The *g* values were measured with respect to diphenylpicrylhydrazyl (*g* = 2.0036 ± 0.0003).

Cyclic voltammetry was carried out with an EG&G model 173 potentiostat or an IBM model EC 225 voltammetric analyzer. A three-electrode system was used and consisted of a glassy carbon or platinum disk working electrode, a platinum wire counter electrode, and a saturated calomel electrode (SCE) as the reference electrode. The SCE was separated from the bulk of the solution by a fritted-glass bridge of low porosity which contained the solvent/supporting electrolyte mixture. All potentials are referenced to the SCE. UV-visible spectroelectrochemical experiments were carried out with a Hewlett-Packard model 8453 diode array spectrophotometer. UV-visible spectra were recorded on a Perkin-Elmer Lambda 7 spectrophotometer, and IR measurements were performed with a Perkin-Elmer IR 283 or a Perkin-Elmer Series 1600 spectrophotometer. Electron ionization mass spectra were obtained on a Finnigan 3200 or Finnigan MAT 212 instrument. Elemental analyses were provided by Bayer AG, Leverkusen, Germany.

Chemicals. Benzonitrile (PhCN) was purchased from Aldrich Chemical Co. and distilled over P₂O₅ under vacuum prior to use. Absolute dichloromethane (CH₂Cl₂) and CDCl₃ (for NMR measurements) were obtained from Aldrich also and used as received. Tetra-*n*-butylammonium perchlorate was purchased from Sigma Chemical Co., recrystallized from ethyl alcohol, and dried under vacuum at 40 °C for at least 1 week prior to use. The investigated compounds were synthesized as described below.

(OEC)As. To a solution of 523 mg (1 mmol) of octaethylcorrole in 20 mL of pyridine was added 1 mL of arsenic trichloride. After 5 min, the volatile compounds were removed in vacuo. The residue was passed through a short column of alumina (Brockmann) using CH₂Cl₂ as the eluent. The green band that formed contained the arsenic corrole, which was obtained after crystallization from dichloromethane/methanol as violet needles with a metallic luster (yield: 560 mg, 94%). ¹H NMR (300 MHz, CDCl₃): $\delta = 9.69$ (singlet, 2 H, H-5,15), 9.50 (singlet, 1 H, H-10), 4.21–3.97 (multiplets, 16 H, CH₂), 1.93 (triplet, 6 H, CH₃), 1.88 (triplet, 6 H, CH₃), 1.86 (triplet, 12 H, CH₃). ¹³C NMR (75.5 MHz, CDCl₃): $\delta = 139.38, 138.69, 138.05, 136.18, 134.50, 133.00, 128.60, 91.54$ (C-10), 86.60 (C-5,15), 20.64, 19.92, 19.63, 18.83, 18.69, 18.18, 18.04. MS (EI, 70 eV): *m/z* (%) 594 (100) M⁺, 579 (10) [M - CH₃]⁺, 564 (6) [M - 2CH₃]⁺, 549 (12) [M - 3CH₃]⁺, 297 (33) [M]²⁺, 282 (18) [M - 2CH₃]²⁺. IR (CsI): $\nu = 2962, 2926, 2867, 1497, 1470, 1445, 1372, 1188, 1158, 1056, 1012, 1003, 957, 800$ cm⁻¹. UV-vis (CH₂Cl₂): λ_{\max} (nm) (10⁻⁴ ε (mol⁻¹ L cm⁻¹)) = 325 (3.7), 377 (2.0), 407 (1.0), 443 (9.7), 453 (8.0), 554 (1.0), 589 (1.5), 624 (1.2). Anal.

Calcd for C₃₅H₄₃N₄As: C, 70.69; H, 7.29; N, 9.42. Found: C, 70.81; H, 7.24; N, 9.55.

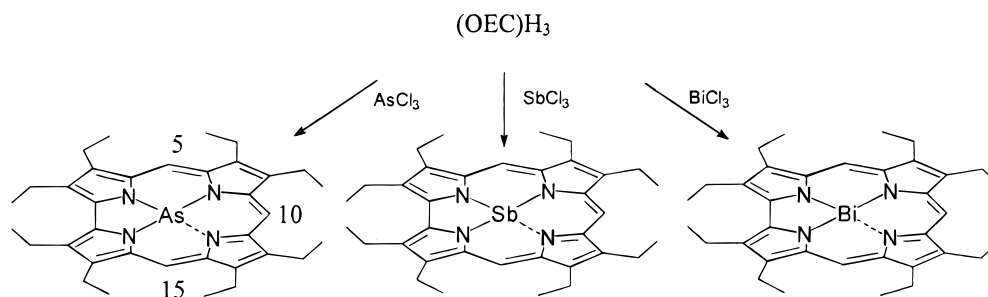
(OEC)Sb. A mixture of 523 mg (1 mmol) of octaethylcorrole and 1 g of antimony trichloride in 20 mL of pyridine was heated to 100 °C for 5 min, after which the volatile compounds were removed in vacuo. The residue was passed through a short column of alumina (Brockmann) using dichloromethane as the eluent. The green band that formed contained the antimony corrole, which was obtained after crystallization from dichloromethane/methanol as violet needles with a metallic luster (yield: 575 mg, 90%). ¹H NMR (300 MHz, CDCl₃): $\delta = 9.70$ (singlet, 2 H, H-5,15), 9.49 (singlet, 1 H, H-10), 4.18–3.95 (multiplets, 16 H, CH₂), 1.90 (triplet, 6 H, CH₃), 1.87 (triplet, 6 H, CH₃), 1.84 (triplet, 6 H, CH₃), 1.83 (triplet, 6 H, CH₃). ¹³C NMR (75.5 MHz, CDCl₃): $\delta = 140.11, 139.31, 138.89, 136.53, 135.44, 134.64, 131.56, 131.06, 93.22$ (C-10), 87.29 (C-5,15), 20.73, 19.92, 19.92, 19.64, 18.91, 18.70, 18.23, 18.01. MS (EI, 70 eV): *m/z* (%) 640 (100) M⁺, 625 (6) [M - CH₃]⁺, 610 (5) [M - 2CH₃]⁺, 320 (9) [M]²⁺, 305 (5) [M - 2CH₃]²⁺. IR (CsI): $\nu = 2961, 2926, 2866, 1481, 1464, 1452, 1188, 1154, 1056, 1010, 959, 801$ cm⁻¹. UV-vis (CH₂Cl₂): λ_{\max} (nm) (10⁻⁴ ε (mol⁻¹ L cm⁻¹)) = 319 (3.7), 361 (1.8), 419 (2.3) sh, 440 (12.9), 446 (11.0) sh, 548 (0.8), 588 (2.1), 617 (1.5).

(OEC)Bi. A mixture of 523 mg (1 mmol) of octaethylcorrole, 1 g of bismuth trichloride, and 1 g potassium acetate in 20 mL of DMF was refluxed for 20 min under an argon atmosphere, after which diethyl ether was added and the organic layer was washed thoroughly with water. After removal of the volatile compounds, the residue was passed through a short column of alumina (Brockmann) using 1/1 diethyl ether/hexane as the eluent. The green fraction contained the bismuth complex, which was obtained after crystallization from dichloromethane/methanol as a violet powder (yield: 595 mg, 82%). ¹H NMR (300 MHz, CDCl₃): $\delta = 9.53$ (singlet, 2 H, H-5,15), 9.31 (singlet, 1 H, H-10), 4.13–3.91 (multiplets, 16 H, CH₂), 1.82 (triplet, 6 H, CH₃), 1.81 (triplet, 6 H, CH₃), 1.78 (triplet, 6 H, CH₃), 1.76 (triplet, 6 H, CH₃). ¹³C NMR (75.5 MHz, CDCl₃): $\delta = 140.84, 139.34, 137.39, 136.99, 136.70, 135.28, 134.91, 131.77, 97.74$ (C-10), 88.53 (C-5,15), 20.74, 19.97, 19.81, 19.67, 19.03, 18.74, 18.35, 18.10. MS (EI, 70 eV): *m/z* (%) 728 (100) M⁺, 713 (7) [M - CH₃]⁺, 698 (5) [M - 2CH₃]⁺, 684 (8) [M - 3CH₃]⁺, 364 (15) [M]²⁺, 349 (8) [M - 2CH₃]²⁺. IR (CsI): $\nu = 2963, 2929, 2868, 1464, 1448, 1376, 1186, 1154, 1057, 1010, 958, 796$ cm⁻¹. UV-vis (CH₂Cl₂): λ_{\max} (nm) (10⁻⁴ ε (mol⁻¹ L cm⁻¹)) = 320 (3.1), 411 (2.5), 447 (6.3), 557 (0.9), 592 (1.9), 612 (1.3).

[(OEC)As(CH₃)⁺ClO₄⁻]. A solution containing 595 mg (1 mmol) of (OEC)As, 5 mL of methyl iodide, 15 mL of THF, and 0.5 g of potassium carbonate was stirred for 48 h in the absence of light. The volatile compounds were removed in vacuo, after which the residue was passed through a column of alumina using first dichloromethane (to elute traces of the starting compound) and then diethyl ether as the eluent. The purple eluate was collected and evaporated to dryness. The residue was solubilized in a mixture of dichloromethane/methanol (1/1) containing perchloric acid, and the dichloromethane was removed by gentle heating in a water bath. After crystallization at -20 °C, the product was obtained as red cubes, which were washed with water and dried in vacuo. Yield: 585 mg (83%). **Caution!** Organic perchlorate salts can detonate spontaneously. Although no explosions were encountered in this work, precautions are warranted. The preparation of (OEC)As(CH₃)ClO₄ was always done on a small scale, and the material was not stored for long periods. ¹H NMR (300 MHz, CDCl₃): $\delta = 10.15$ (singlet, 2 H, H-5,15), 10.10 (singlet, 1 H, H-10), 4.33–4.07 (multiplets, 16 H, CH₂), 1.96 (triplet, 6 H, CH₃), 1.92 (triplet, 6 H, CH₃), 1.91 (triplet, 6 H, CH₃), 1.90 (triplet, 6 H, CH₃), -3.76 (singlet, 3 H, As-CH₃). ¹³C NMR (75.5 MHz, CDCl₃): $\delta = 142.69, 140.22, 137.97, 136.75, 136.31, 133.63, 132.94, 125.06, 93.62$ (C-5), 90.51 (C-5,15), 20.65, 20.06, 20.06, 19.70 (As-CH₃), 19.65, 18.26, 18.24, 17.68, 17.59. MS (EI, 70 eV): *m/z* (%) 609 (100) M⁺, 594 (53) [M - CH₃]⁺, 579 (18) [M - 2CH₃]⁺, 564 (15) [M - 3CH₃]⁺. IR (CsI): $\nu = 2965, 2933, 2873, 1506, 1465, 1193, 1163, 1151, 1099, 1087, 1060, 1020, 1012, 967, 624$ cm⁻¹. UV-vis (CH₂Cl₂): λ_{\max} (nm) (10⁻⁴ ε (mol⁻¹ L cm⁻¹)) = 281 (1.8) sh, 362 (1.4) sh, 390 (6.4) sh, 407 (18.1), 492 (0.5), 531 (1.6), 565 (2.7). Anal. Calcd for C₃₆H₄₆N₄-

- (24) Marrese, C. A.; Carrano, C. J. *Inorg. Chem.* **1984**, *23*, 3961.
 (25) (a) Satoh, W.; Nadano, R.; Yamamoto, G.; Yamamoto, Y.; Akiba, K.-y. *Organometallics* **1997**, *16*, 3664. (b) Goh, G. K.; Czuchajowski, L. J. *Porphyrins Phthalocyanines* **1997**, *3*, 281–285. (c) Yasumoto, M.; Satoh, W.; Nadano, R.; Yamamoto, Y.; Akiba, K.-y. *Chem. Lett.* **1999**, *8*, 791.
 (26) Vangberg, T.; Ghosh, A. *J. Am. Chem. Soc.* **1999**, *121*, 12154.
 (27) Segewa, H.; Kunimoto, K.; Nakamoto, A.; Shimidzu, T. *J. Chem. Soc., Perkin Trans. 1* **1992**, 939.
 (28) Yamamoto, Y.; Nadano, R.; Itagaki, M.; Akiba, K.-y. *J. Am. Chem. Soc.* **1995**, *117*, 8287.
 (29) Michaudet, L.; Fasseur, D.; Guillard, R.; Ou, Z.; Kadish, K. M.; Dahanoui, S.; Lecomte, C. *J. Porphyrins Phthalocyanines* **2000**, *4*, 261–270.

Scheme 1

**Table 1.** Selected ^1H NMR Data for Group 15 Octaethylcorroles (ppm)

compound	ligand CH_3	macrocycle			
		H-5,15	H-10	CH_2	CH_3
(OEC)As		9.69	9.50	4.21–3.97	1.93–1.86
(OEC)Sb		9.70	9.49	4.18–3.95	1.90–1.83
(OEC)Bi		9.53	9.31	4.13–3.91	1.82–1.76
$[(\text{OEC})\text{As}(\text{CH}_3)]^+\text{ClO}_4^-$	-3.76	10.15	10.10	4.33–4.07	1.96–1.90

AsClO_4 : C, 60.97; H, 6.54; N, 7.90; Cl, 5.00. Found: C, 60.96; H, 5.93; N, 8.13; Cl, 5.02.

Results and Discussion

Synthesis of (OEC)As, (OEC)Sb, and (OEC)Bi. The group 15 elements were incorporated into the octaethylcorrole macrocycle by reaction of the free-base corrole with the element(III) chlorides in basic solvents followed by conventional workup. This reaction is shown in Scheme 1 and yields, in each case, the corrole complex containing a trivalent central ion, i.e., (OEC)M where M = As(III), Sb(III), or Bi(III).

All of the main group corroles are stable in the solid state. However, in solution, (OEC)As and (OEC)Sb are slowly converted by oxygen into compounds which have UV–visible spectra similar to that of $[(\text{OEC})\text{As}^{\text{V}}(\text{CH}_3)]^+$ (see following sections), and it can be concluded that a M(III)/M(V) oxidation has taken place. It is noteworthy to point out that this oxidation process is strongly accelerated by light. Attempts to chemically oxidize (OEC)Bi^{III} to its Bi(V) form resulted only in unspecific decomposition products. The (OEC)As and (OEC)Sb corroles are demetalated in solution by concentrated hydrochloric acid, and (OEC)Bi is far more acid sensitive than are the As and Sb complexes. The free-base corrole is formed during chromatography of (OEC)Bi on silica gel using chlorinated hydrocarbons.

The ^1H NMR spectra of (OEC)As, (OEC)Sb, and (OEC)Bi are similar and show characteristic features of diamagnetic aromatic compounds (see Table 1). The meso protons H-5,15

and H-10 of these complexes have resonances in the region $\delta = 9.70\text{--}9.31$, confirming a strong diamagnetic ring current effect. The protons of the CH_2 units of all corroles give rise to multiplets (the AB part of an ABX_3 spin system) around 4 ppm. This diastereotopism indicates the lack of a horizontal symmetry plane and leads to the conclusion that the central ions of the M(III) corroles each adopt an out-of-plane position. The CH_2 and CH_3 proton signals of (OEC)As and (OEC)Sb show little dependence on the metal ion and resonate at very similar fields (see Table 1), while both signals for (OEC)Bi are upfield-shifted compared to those of the As(III) and Sb(III) complexes.

Synthesis of $[(\text{OEC})\text{As}^{\text{V}}(\text{CH}_3)]^+\text{ClO}_4^-$. The σ -bonded methyl As(V) corrole, $[(\text{OEC})\text{As}(\text{CH}_3)]^+$, was obtained by oxidative methylation of (OEC)As using methyl iodide. The perchlorate salt was obtained by treatment of the above reaction product with perchloric acid. An oxidative methylation reaction did not occur in the case of either (OEC)Sb or (OEC)Bi.

The formulation of the arsenic methylation product as containing CH_3 bound to the central ion is proven by the NMR spectrum, which indicates the presence of an aromatic compound with C_s symmetry. The meso-proton resonances of $[(\text{OEC})\text{As}(\text{CH}_3)]^+\text{ClO}_4^-$ appear as two singlets at $\delta = 10.15\text{--}10.10$, while the CH_2 units of the ethyl groups correspond to multiplets at $\delta = 4.33\text{--}4.07$. The resonance of the methyl group bound to the central ion occurs at high field. A singlet at $\delta = -3.76$ is found for the σ -bonded methyl ligand of $[(\text{OEC})\text{As}(\text{CH}_3)]^+\text{ClO}_4^-$ (Table 1). The strong shielding seen for the methyl protons is a result of the magnetic anisotropy of the aromatic corrole macrocycle. The resonances of the corrole protons in $[(\text{OEC})\text{As}(\text{CH}_3)]^+\text{ClO}_4^-$ are shifted to lower fields as compared to those in neutral (OEC)As, and this is due to the presence of a positive charge in the As(V) derivative.

UV–Visible Spectra. The UV–visible data for the investigated corroles and related porphyrins with the same metal ions are given in Table 2. On the basis of the shapes and positions

Table 2. UV–Visible Data for Arsenic, Antimony, and Bismuth Octaethylcorroles in PhCN Containing 0.1 M TBAP and Related Porphyrins^a

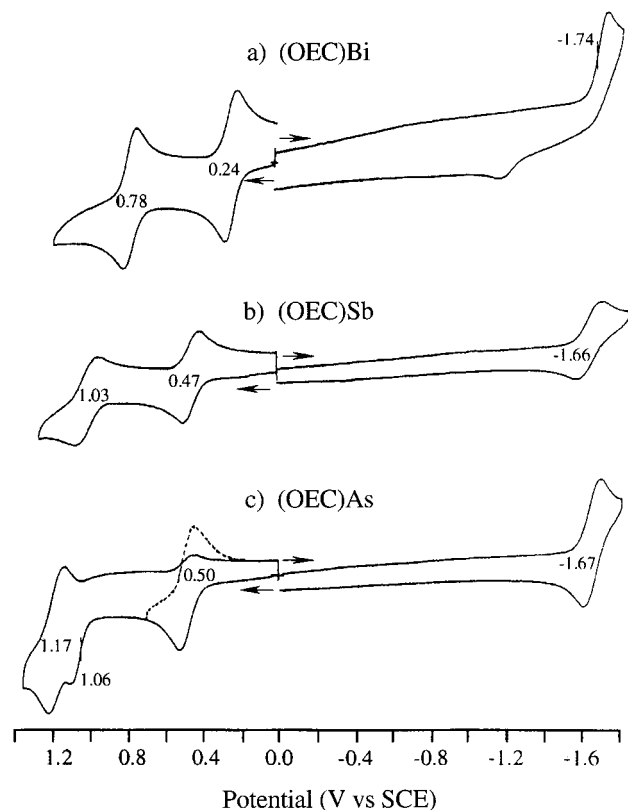
complex	λ_{max} , nm ($10^{-4}\epsilon$, $\text{mol}^{-1}\text{L cm}^{-1}$)						ref
(OEC)As ^{III}	328 (2.4)	379 (1.3)	445 (7.3) ^b	551 (0.6)	590 (1.0)	623 (0.8)	tw
(OEC)Sb ^{III}	322 (2.9)	366 (1.6)	442 (10.5)	549 (0.9)	589 (1.8)	616 (1.3)	tw
(OEC)Bi ^{III}	319 (2.3)	418 ^c (2.1)	449 (5.6)	557 (0.7)	594 (1.6)	615 (1.1)	tw
$[(\text{OEC})\text{As}^{\text{V}}(\text{CH}_3)]^+$	307 (1.0)	388 ^c (4.3)	409 (13.8)	531 (1.2)	565 (2.0)		tw
(TPP)Sb ^{III} Cl	357 (4.2)	378 ^c (2.6)	438 ^c (2.3)	465 (12.0)	594 (0.4)	644 (1.0)	20 ^c
(OEP)Sb ^{III} Cl	355 ^c (3.0)	376 (6.4)	430 ^c (2.1)	460 (4.6)	570 (0.9)	600 ^c (0.3)	20 ^c
(TPP)Bi ^{III} (SO_3CF_3)		348 (5.5)	470 (17.4)	599 (1.0)	647 (1.2)		29 ^d
(TMP)Bi ^{III} (SO_3CF_3)		345 (5.2)	472 (15.1)	602 (1.1)	648 (1.2)		29 ^d
$[(\text{TPP})\text{Sb}^{\text{V}}(\text{CH}_3)_2]^+$		347 (2.0)	439 (32.0)	580 (1.0)	623 (2.3)		23 ^e
$[(\text{OEP})\text{As}^{\text{V}}(\text{CH}_3)_2]^+$		366 (4.0)	424 (28.2)	551 (1.7)	585 (0.7)		25 ^f

^a Superscript “s” = shoulder; tw = this work. ^b A small peak also can be seen at 411 nm. ^c Spectral data for other Sb(III) porphyrins can also be found in this reference. TPP = tetraphenylporphyrin dianion; OEP = octaethylporphyrin dianion. ^d Spectral data for other Bi(III) porphyrins can also be found in this reference. TMP = tetramesitylporphyrin dianion. ^e Spectral data for other Sb(V) porphyrins can also be found in this reference. ^f Spectral data for other As(V) porphyrins can also be found in this reference.

Table 3. Half-Wave Potentials (V vs SCE) in PhCN, 0.1 TBAP^a

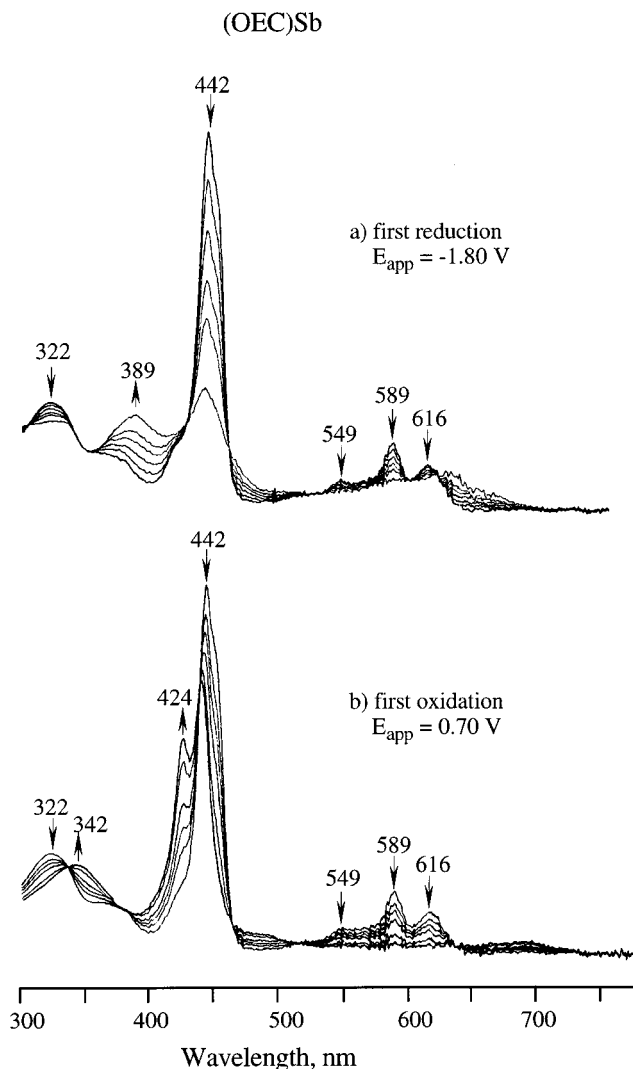
compound	oxidation				reduction	
	4th	3rd	2nd	1st		
(OEC)As ^{III}	(1.48) ^b	(1.17) ^b	1.09 ^c	0.50		-1.67
(OEC)Sb ^{III}		1.36 ^c	1.03	0.47		-1.66
(OEC)Bi ^{III}		1.47 ^c	0.78	0.24		1.77 ^c
[(OEC)As ^V (CH ₃) ₂] ⁺ ClO ₄ ⁻	1.59	1.16		(0.48) ^d	-1.01 ^c	(-1.61) ^e

^a Values for product of species generated from a chemical reactions following electron transfer are shown in parentheses. ^b The process involves the As(V) corrole generated from the chemical reaction following the second oxidation. ^c Peak potential at a scan rate of 0.1 V/s. ^d Process involves oxidation of the As(III) corrole generated from the chemical reaction following the first reduction. ^e The process involves the reduction of the As(III) corrole generated from the chemical reaction following the first reduction (see text).

**Figure 1.** Cyclic voltammograms of (a) (OEC)Bi, (b) (OEC)Sb, and (c) (OEC)As in PhCN containing 0.1 M TBAP. Scan rate = 0.1 V/s.

of the Soret bands, the examined neutral corroles can be divided into two groups. The first are those with formally trivalent central ions, i.e., (OEC)As, (OEC)Sb, and (OEC)Bi, each of which shows a hyper type of absorption spectrum, while the second group of compounds is represented by [(OEC)As^V(CH₃)₂]⁺ClO₄⁻, which exhibits a normal type of UV-visible spectrum with a single Soret band having an absorption maximum at 409 nm. As will be later demonstrated, a third type of spectrum is also seen for [(OEC)As^{IV}]⁺ and [(OEC)Sb^{IV}]⁺. The spectra of these M(IV) species each have a split Soret band around 425 and 440 nm.

The UV-vis spectra of free-base (OEC)H₃ and (OEP)H₂ are similar.¹ The Soret band of (OEC)H₃ is located at 396 nm, and (OEP)H₂ has a Soret band at 397 nm. However, different types of spectra are seen in the cases of metallocorroles and metalloporphyrins. The Soret bands of the metallocorroles are blue-shifted by 15–20 nm as compared to those of the metalloporphyrins which contain the same metal ions in the same oxidation states (see Table 2). For example, the Soret band of (OEC)Sb^{III} is located at 442 nm, while that of (OEP)Sb^{III}Cl is located at 460 nm, and the Soret and visible bands of [(OEC)As^V(CH₃)₂]⁺

**Figure 2.** UV-visible spectral changes during controlled-potential electrolysis of (OEC)Sb at (a) -1.80 V and (b) 0.70 V in PhCN, 0.1 M TBAP.

are located at 409, 531, and 565 nm, while those of [(OEP)As^V(CH₃)₂]⁺ are located at 424, 551, and 585 nm.

Electroreduction of (OEC)As and (OEC)Sb. Cyclic voltammograms of (OEC)As and (OEC)Sb in PhCN containing 0.1 M TBAP are shown in Figure 1, while the electrochemical data are summarized in Table 3. Both compounds undergo single reversible one-electron reductions which occur at $E_{1/2} = -1.67$ V for (OEC)As and -1.66 V for (OEC)Sb. The reductions of both corroles are ring-centered, leading to As(III) and Sb(III) corrole π -anion radicals, as ascertained from the UV-visible spectral changes shown in Figure 2a.

Electrooxidation of (OEC)As and (OEC)Sb. The first oxidations of (OEC)As and (OEC)Sb involve reversible one-

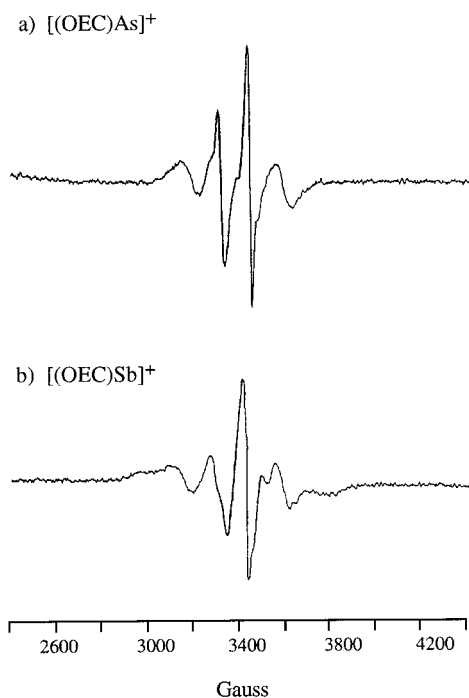


Figure 3. ESR spectra obtained after one-electron oxidation with 1 equiv of AgClO_4 for (a) $(\text{OEC})\text{As}$ and (b) $(\text{OEC})\text{Sb}$ in PhCN at 77 K.

electron-transfer processes which occur at $E_{1/2} = 0.50$ V for $(\text{OEC})\text{As}$ and 0.47 V for $(\text{OEC})\text{Sb}$ (see Figure 1 and Table 3) and are accompanied by UV–visible spectral changes of the type shown in Figure 2b for the case of $(\text{OEC})\text{Sb}$.

The same one-electron-oxidation products are obtained after bulk electrolyses of $(\text{OEC})\text{As}$ and $(\text{OEC})\text{Sb}$ in PhCN at $E_{\text{app}} = 0.70$ V or after chemical oxidations with 1 equiv of AgClO_4 . The ESR spectra of the latter chemical oxidation products are shown in Figure 3. Singly oxidized $[(\text{OEC})\text{As}]^+$ exhibits an almost isotropic spectrum centered at $g = 2.01$ with a large hyperfine splitting on the $I = 3/2$ As nucleus ($a = 133$ G). Singly oxidized $[(\text{OEC})\text{Sb}]^+$ exhibits a spectrum centered at $g = 2.01$ with hyperfine splittings on the $I = 5/2$ ^{121}Sb ion and the $I = 7/2$ ^{123}Sb ion. These ESR data thus indicate that the unpaired electron of each one-electron-oxidized species is mainly localized on the central ion rather than on the corrole macrocycle, and the products of the one-electron oxidations are then best represented as $[(\text{OEC})\text{As}^{\text{IV}}]^+$ and $[(\text{OEC})\text{Sb}^{\text{IV}}]^+$. Under these conditions, the first electron-transfer reaction of each $(\text{OEC})\text{M}$ species must involve a reversible metal-centered $\text{M}(\text{III})/\text{M}(\text{IV})$ transition. No changes were seen in the shapes of the ESR signals for $[(\text{OEC})\text{As}^{\text{IV}}]^+$ and $[(\text{OEC})\text{Sb}^{\text{IV}}]^+$ over a temperature range between 77 and 150 K in frozen PhCN. The ESR spectrum of $[(\text{OEC})\text{Sb}^{\text{IV}}]^+$ is also similar to a spectrum reported for a singly reduced antimony(V) porphyrin which was assigned to an antimony(IV) species.²¹

The second one-electron oxidation of $(\text{OEC})\text{As}$ is irreversible and located at $E_{\text{pa}} = 1.09$ V. This irreversible oxidation is followed by a reversible one-electron-transfer process at $E_{1/2} = 1.17$ V and a quasi-reversible process at $E_{1/2} = 1.48$ V (see Figure 4). UV–visible spectral changes obtained after thin-layer controlled-potential electrolysis of $(\text{OEC})\text{As}$ at 1.10 V (the second oxidation) are shown in Figure 5c. The final product of the oxidation has a Soret band located at 401 nm and two visible bands at 524 and 560 nm. This spectrum is similar to the spectrum of $[(\text{OEC})\text{As}(\text{CH}_3)]^+$, which contains As(V). The latter spectrum is shown as an inset in Figure 5c. These results suggest that the two-electron oxidation product of $(\text{OEC})\text{As}$ is an

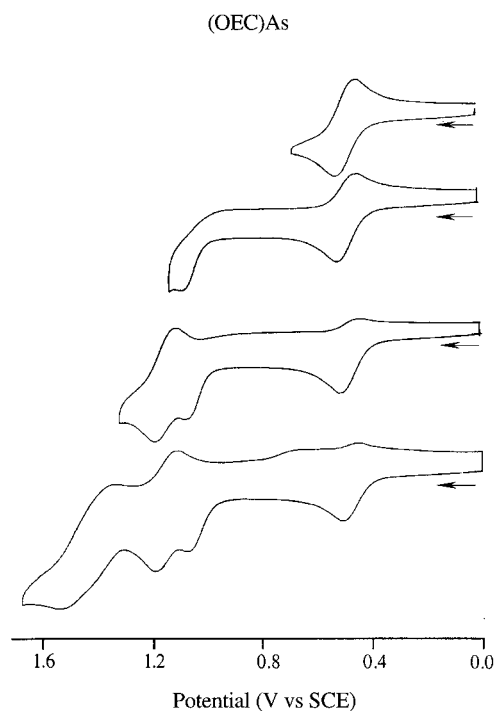


Figure 4. Cyclic voltammograms of $(\text{OEC})\text{As}$ in PhCN, 0.1 M TBAP, showing four oxidation processes. See text for details.

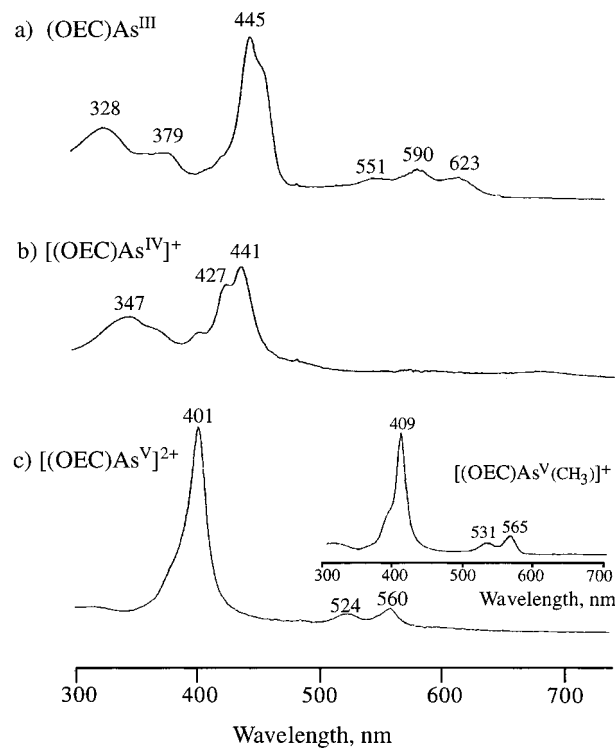
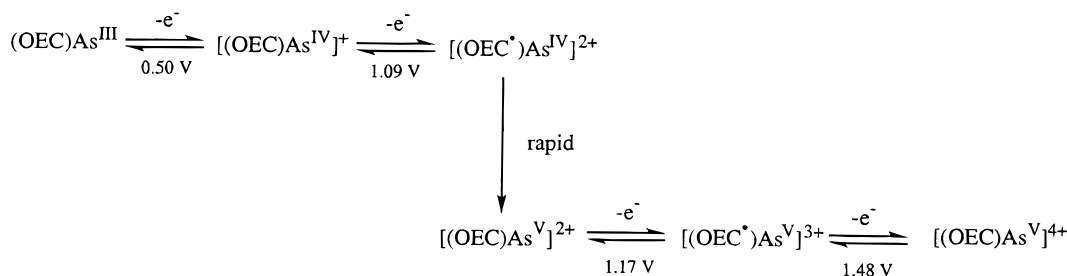


Figure 5. UV–visible spectra of (a) neutral $(\text{OEC})\text{As}$, (b) electrochemically generated $[(\text{OEC})\text{As}^{\text{IV}}]^+$ after the first oxidation, and (c) electrochemically generated $[(\text{OEC})\text{As}^{\text{V}}]^{2+}$ after the second oxidation, with a comparison to the spectrum of $[(\text{OEC})\text{As}^{\text{V}}(\text{CH}_3)]^+\text{ClO}_4^-$, which is shown as an inset. Medium: PhCN, 0.1 M TBAP.

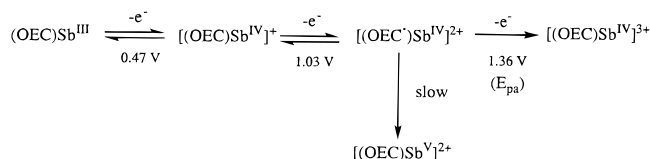
arsenic(V) corrole, and the two additional oxidations seen at $E_{1/2} = 1.17$ and 1.48 V are then assigned to the stepwise formation of an arsenic(V) corrole π -cation radical and dication as shown in Scheme 2.

The second and third oxidations of $(\text{OEC})\text{Sb}$ are reversible and are located at $E_{1/2} = 1.03$ and $E_{\text{pa}} = 1.36$ V (see Table 3). Spectroelectrochemical data obtained during thin-layer controlled-

Scheme 2



Scheme 3



potential oxidation indicate that the process at 1.03 V corresponds to the formation of $[(\text{OEC}^\bullet)\text{Sb}^{\text{IV}}]^{2+}$, which is slowly converted to $[(\text{OEC})\text{Sb}^{\text{V}}]^{2+}$. The third electrode reaction at $E_{\text{pa}} = 1.36 \text{ V}$ therefore corresponds to the formation of $[(\text{OEC})\text{Sb}^{\text{IV}}]^{3+}$ as shown in Scheme 3.

Electrochemistry of $[(\text{OEC})\text{As}(\text{CH}_3)]^+\text{ClO}_4^-$. The cyclic voltammograms of $[(\text{OEC})\text{As}(\text{CH}_3)]^+\text{ClO}_4^-$ are shown in Figure 6a,b, while Figure 6c shows the voltammogram of $(\text{OEC})\text{As}$, all in PhCN containing 0.1 M TBAP. The methylarsenic(V) complex (Figure 6a) undergoes an initial oxidation at $E_{1/2} = 1.16 \text{ V}$ and two reductions at $E_{\text{pc}} = -1.01 \text{ V}$ and $E_{1/2} = -1.61 \text{ V}$. The one-electron oxidation of $[(\text{OEC})\text{As}(\text{CH}_3)]^+\text{ClO}_4^-$ leads to an As(V) corrole π -cation radical, while the first reduction of the same compound at $E_{\text{pc}} = -1.01 \text{ V}$ involves an irreversible one-electron transfer and results in the formation of a product that can be reversibly oxidized at $E_{1/2} = 0.48 \text{ V}$ (see Figures 6b and 7a). This electrode process is not observed upon initial scans in a positive direction (see Figure 6a).

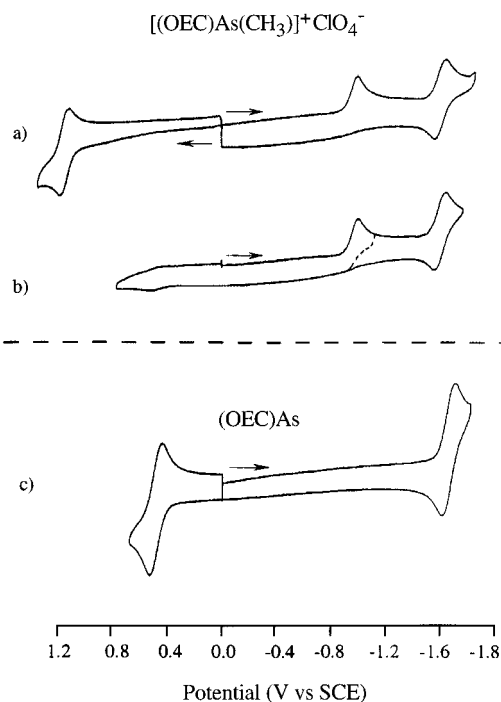


Figure 6. Cyclic voltammograms of $[(\text{OEC})\text{As}^{\text{V}}(\text{CH}_3)]^+\text{ClO}_4^-$ and $(\text{OEC})\text{As}$ in PhCN, 0.1 M TBAP.

Scheme 4

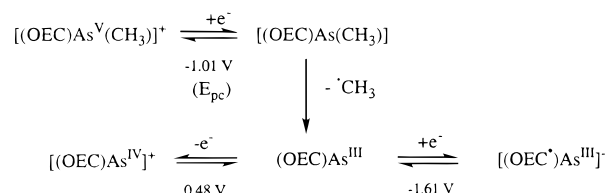


Figure 7 shows the thin-layer cyclic voltammograms of $[(\text{OEC})\text{As}(\text{CH}_3)]^+\text{ClO}_4^-$ and the corresponding UV–visible spectra before (---) and after (—) controlled-potential reduction at -1.30 V . Figures 6 and 7 clearly indicate that the electroreduction of $[(\text{OEC})\text{As}(\text{CH}_3)]^+\text{ClO}_4^-$ is followed by a chemical reaction which results in the formation of $(\text{OEC})\text{As}$. A plausible mechanism for this reaction involves the initial formation of an arsenic(V) corrole π -anion radical, $[(\text{OEC})\text{As}^{\text{V}}(\text{CH}_3)]^{\bullet-}$, which then rapidly undergoes internal electron transfer and dissociation of $\cdot\text{CH}_3$, with formation of $(\text{OEC})\text{As}$, as shown in Scheme 4. The electrode reaction at $E_{1/2} = 0.48 \text{ V}$ in Figures 6 and 7 thus corresponds to the first one-electron oxidation of homogeneously generated $(\text{OEC})\text{As}$ as discussed above.

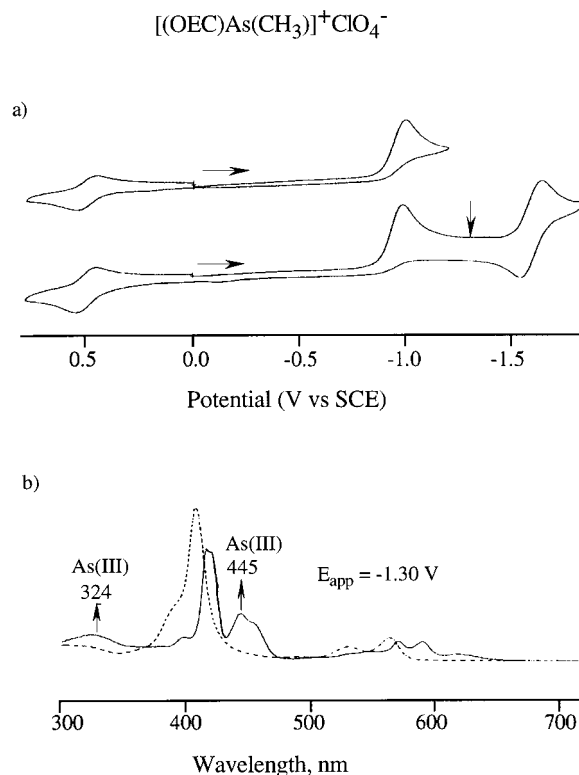


Figure 7. (a) Thin-layer cyclic voltammograms of $[(\text{OEC})\text{As}^{\text{V}}(\text{CH}_3)]^+\text{ClO}_4^-$ and (b) UV–visible spectral changes of the same compound before (---) and after (—) the first controlled-potential reduction at -1.30 V in PhCN, 0.1 M TBAP.

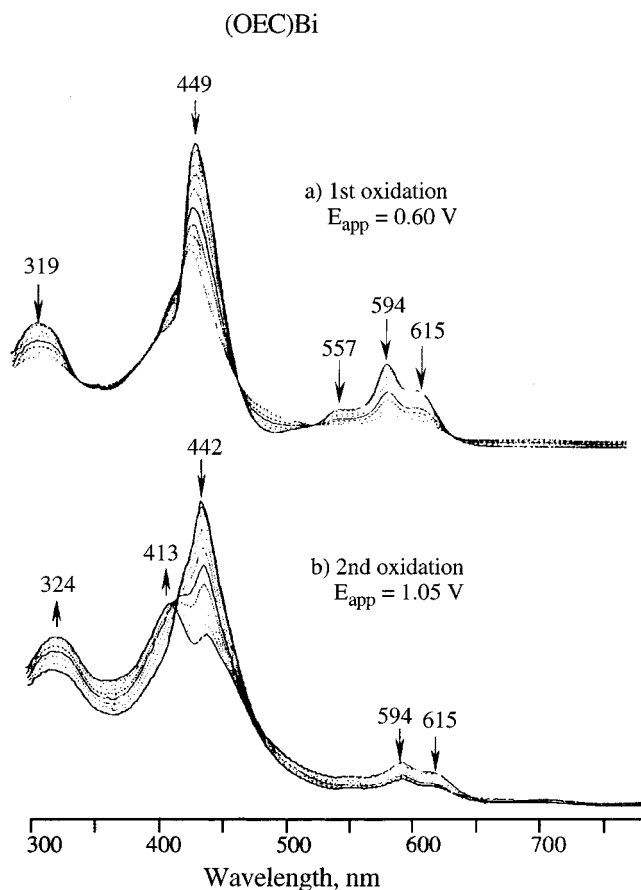


Figure 8. UV-visible spectral changes of (OEC)Bi during controlled-potential oxidations at (a) 0.60 V and (b) 1.05 V in PhCN, 0.1 M TBAP.

The conversion of $[(\text{OEC})\text{As}(\text{CH}_3)]^+\text{ClO}_4^-$ (dashed line in Figure 7) to (OEC)As (solid line in Figure 7) is confirmed by thin-layer spectroelectrochemistry, which shows the appearance, after reduction, of a new absorption band at 445 nm that is characteristic of neutral (OEC)As.

Electrochemistry of (OEC)Bi. The electroreduction of (OEC)Bi in PhCN containing 0.1 M TBAP differs from that of (OEC)As and (OEC)Sb in its irreversibility ($E_{\text{pc}} = -1.77$ V). A reoxidation peak at $E_{\text{pa}} = -1.22$ V is observed after the first reduction (Figure 1a), and this value is close to the first reduction

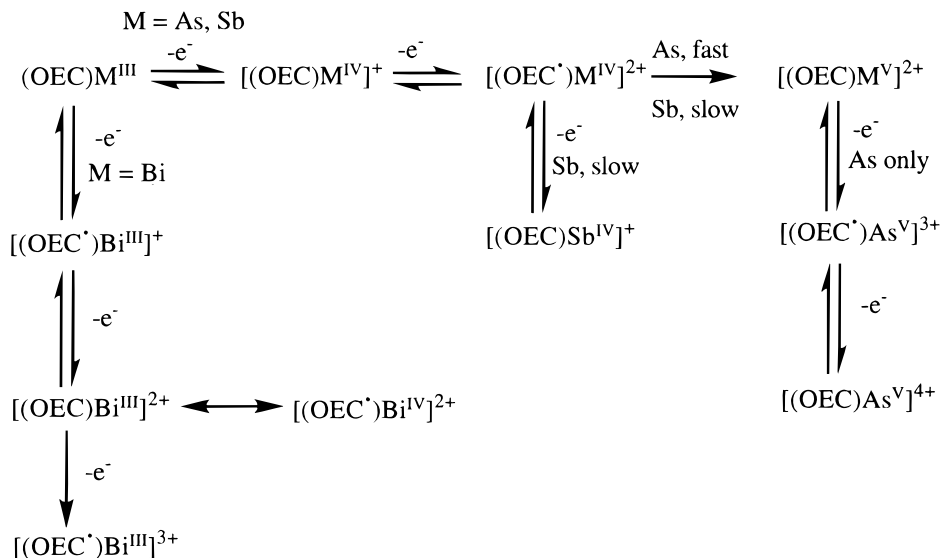
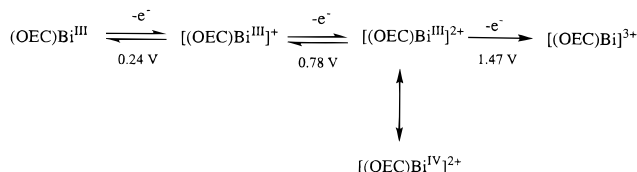


Figure 9. Overall mechanisms for the oxidation of (OEC)M complexes in PhCN.

Scheme 5



potential of free-base 7,8,12,13-tetramethyl-2,3,10,17,18-pentaphenylcorrole ($E_{\text{pa}} = -1.32$ V) which was measured under the same experimental conditions. Thus, the most plausible explanation for this irreversibility is a demetalation of the corrole after formation of the corrole π -anion radical.

The first reversible oxidation of (OEC)Bi at $E_{1/2} = 0.24$ (Figure 1a) is assigned to the formation of a Bi(III) corrole π -cation radical on the basis of spectroelectrochemical data (Figure 8a). The intensity of the Soret band decreases during the second oxidation while a new blue-shifted band at 413 nm appears (Figure 8b). This result is similar to that obtained after the first oxidations of (OEC)Sb and (OEC)As (Figures 2b and 5b), thus indicating that a Bi(IV) species is slowly generated in solution. A third irreversible oxidation of the compound is also observed at $E_{\text{pa}} = 1.47$ V, and the proposed electrooxidation mechanism is shown in Scheme 5.

Comparisons between Electrochemical Properties of Investigated Corroles and Related Porphyrins. Several comparisons have been made between the redox behavior of corroles and porphyrins, with the majority of studies involving complexes of iron,³⁰ cobalt,^{31,32} and tin.¹⁴ A comparison between the electrochemistry of octaethylcorroles described in this paper and that of related octaethylporphyrins with group 15 ions shows that the σ -bonded As(V) octaethylcorrole can be converted to an As(III) product after electroreduction and loss of the axial ligand, which is not the case for As(V) octaethylporphyrins that are reduced to porphyrin π -anion radicals and dianions.³³ However, it should be noted that Sb(III) porphyrin products can be slowly formed after electroreduction of some, but not all, Sb(V) octaethylporphyrins which are initially reduced at the conjugated macrocycles to give Sb(V) porphyrin π -anion radicals.^{21,23} The first electrooxidation is invariably macrocycle-centered for Bi(III) corroles and porphyrins,²⁹ but this is not the case for Sb(III) and As(III) corroles, where the first one-

electron oxidation is metal-centered for the corroles and ring-centered for the porphyrins.³⁴

A summary of the overall oxidation mechanisms for (OEC)M, where M = As, Sb, and Bi, is given in Figure 9. Each compound undergoes one reduction and two to four oxidations, with the site of electron transfer and redox potentials depending upon the specific element and its electronegativity which varies from 1.67 for Bi to 1.82 for Sb to 2.20 for As.³⁵ The corrole easiest to oxidize is (OEC)Bi, which is converted to its π -cation radical form, [(OEC)Bi]⁺, at 0.48 V, while the corrole most difficult to oxidize is (OEC)As, which is converted to its As(IV) and As(V) forms at $E_{1/2} = 0.50$ V and $E_{pa} = 1.09$ V prior to formation of an As(V) π -cation radical and dication at more positive potentials.

The first two oxidations of (OEC)Sb^{III}, occur at potentials quite similar to those for oxidation of (OEC)As^{III} and the corrole

products of the first and second one-electron abstractions are characterized as containing a central ion in the +4 or +5 oxidation states. The most easily electrogenerated M(V) corrole occurs in the case of (OEC)As, while a mixture of [(OEC[•])-Sb^{IV}]²⁺ and [(OEC)Sb^V]²⁺ is seen as a product of the overall two-electron (OEC)Sb electrooxidation. No evidence for [(OEC)-Bi^{IV}]⁺ formation is seen upon the reversible oxidation of (OEC)-Bi, but a second irreversible oxidation leads to a product which is formulated as a Bi(III) dication that is then converted slowly to a Bi(IV) corrole π -cation radical on the thin-layer spectroelectrochemical time scale.

Summary. In conclusion, the investigated group 15 corroles can exist with up to three different oxidation states of the central element. (OEC)As has a formal +3 oxidation state and can be reversibly converted to its As(IV) and As(V) forms, while [(OEC)As(CH₃)]⁺ can be reduced to (OEC)As after addition of one electron and rapid loss of the σ -bonded axial ligand. (OEC)Sb can also be reversibly oxidized to give [(OEC)Sb^{IV}]⁺. An antimony(IV) oxidation state has been observed in the case of reduced Sb(V) porphyrins, but the present paper represents the first example for an electrochemical conversion between three different oxidation states of an arsenic tetrapyrrole.

Acknowledgment. The support of the Robert A. Welch Foundation (K.M.K., Grant E-680) is gratefully acknowledged.

IC991361M

-
- (30) Adamian, V. A. Ph.D. Dissertation, University of Houston, Aug 1995.
(31) Adamian, V. A.; D'Souza, F.; Licoccia, S.; Di Vona, M. L.; Tassoni, E.; Paolesse, R.; Boschi, T.; Kadish, K. M. *Inorg. Chem.* **1995**, *34*, 532.
(32) Kadish, K. M.; Koh, W.; Tagliatesta, P.; D'Souza, F.; Paolesse, R.; Licoccia, S.; Boschi, T. *Inorg. Chem.* **1992**, *31*, 2305.
(33) Kadish, K. M.; Ou, Z.; Tan, X.; Akiba, K.-y.; Satoh, W.; Yamamoto, Y. To be submitted to *Inorg. Chem.*
(34) Fuhrhop, J.-H.; Kadish, K. M.; Davis, D. G. *J. Am. Chem. Soc.* **1973**, *95*, 5140.
(35) Cotton, F. A.; Wilkinson, G. *Advanced Inorganic Chemistry*, 5th ed.; John Wiley & Sons: New York, 1988; p 383.